Electromagnetic Levitation Refining of Silicon–Iron Alloys for Generation of Solar Grade Silicon

Katherine Le, Yindong Yang, Mansoor Barati and Alex McLean

Abstract At present, expensive semiconductor grade silicon (SEG-Si) is used for the manufacture of cells to convert solar energy into electricity. This results in a high cost for photovoltaic electricity compared to electricity derived from conventional sources. The processing of inexpensive metallurgical silicon, or ferrosilicon alloys, is a potentially economical refining route to produce photovoltaic silicon. With phosphorus being one of the most difficult impurities to remove by conventional techniques, this project investigated the use of electromagnetic levitation for dephosphorization of silicon–iron alloy droplets exposed to hydrogen–argon gas mixtures. The effects of time, temperature, hydrogen partial pressure, iron content in the alloy, and initial phosphorus concentration were evaluated.

Keywords Dephosphorization · Electromagnetic levitation · Ferrosilicon · Solar grade silicon · Photovoltaic

Introduction

Solar energy is a promising renewable energy resource for the future with potential to satisfy the growing global energy demand. Silicon is the second most abundant element found in the Earth's crust (27.7%) [1], and the most dominant photovoltaic (PV) material in the industry, comprising the base component of nearly 90% of cells produced [2]. The development of solar grade silicon is hindered by costly and energy intensive production methods, which result in silicon material comprising approximately 45–50% of the total cost of a typical crystalline-silicon module [3]. Current speculation regarding solar energy technology attaining grid parity with

K. Le · Y. Yang (✉) · M. Barati · A. McLean
Department of Materials Science and Engineering, University of Toronto,
184 College St., Toronto, ON M5S 3E4, Canada
e-mail: yindongyang@yahoo.com

M.A. Meyers et al. (eds.), *Proceedings of the 3rd Pan American Materials Congress*,
The Minerals, Metals & Materials Series, DOI 10.1007/978-3-319-52132-9_13

existing electricity technologies, as a result of the recent price decline in solar modules has been partly due to the reduced usage and substitution for silicon materials [3].

The upgrading of inexpensive ferrosilicon alloys or metallurgical grade silicon to solar grade silicon is a potentially economical refining route and several research studies have been carried out. Numerous techniques have been developed to target and remove specific impurity elements in metallurgical silicon alloys, which include: slag refining, acid leaching, solvent refining, solidification refining, and vacuum melting. The investigated methods have been found to be selective, with no single method able to remove all the impurity elements [2]. Phosphorus and boron are deemed as the two most difficult impurity elements to remove from metallurgical silicon by investigated techniques, and have been the focus of several recent studies. In addition to reductions in production costs of SoG-Si, effective removal of the aforementioned impurity elements is essential for producing silicon through metallurgical means [4].

Electromagnetic levitation (EML) refining is an excellent technique for containerless processing of liquid metals. Advantages include the lack of metal contamination from refractory containers, inductive stirring, rapid melting, and approximate spherical geometry of the metal droplet during levitation. The objective of this work is to apply EML to study dephosphorization of ferrosilicon alloys under a hydrogen–argon atmosphere. The effects of time, temperature, hydrogen partial pressure, iron content in the alloy, and initial phosphorus concentration were investigated. Upon achieving effective dephosphorization, the partially refined alloy can be processed by a combination of previously investigated metallurgical techniques into solar grade silicon.

Theoretical Aspects

Phosphorus Removal from Si–Fe Alloy Melts

Evaporative losses of phosphorus (P) in iron (Fe) melts follows the reaction:

$$[\mathrm{P}]_{\mathrm{Fe}} \Leftrightarrow 1/2\mathrm{P}_2(\mathrm{g})$$

Ueda et al. determined the activity coefficient of phosphorus in Si–Fe alloys at a controlled phosphorus partial pressure, showing a maximum value at a certain composition due to strong interaction between silicon and iron. This effect resulted in decreased phosphorus solubility in the alloy. Consequently, the possibility for dephosphorization of silicon alloyed with iron was demonstrated. A value of 0.199 was obtained for the first order interaction parameter e_P^{Fe} for the effect of iron on the activity coefficient of phosphorus [5].

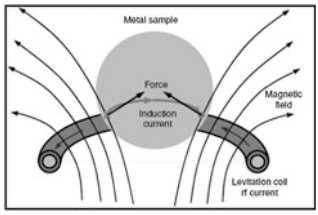

Fig. 1 Electromagnetic levitation principle [9]

From steelmaking data, the interaction parameter for the effect of hydrogen on phosphorus dissolved in an iron melt is $e_P^H = 0.33$ [6]. By using a hydrogen–argon gas mixture, the argon can be considered to produce a vacuum effect, accelerating phosphorus evaporation, while hydrogen in the system generates a reducing atmosphere and increases phosphorus activity in the Si–Fe melt, thus promoting phosphorus removal.

Electromagnetic Levitation Refining

Electromagnetic levitation (EML) is a process that can be utilized for refining molten metals in a containerless environment [7–9]. This prevents potential contamination from impurities while generating inductive stirring [8]. The EML process involves passing an AC electric current through a coil, inducing an eddy current in the conductive sample, which in turn, is melted by heating from the induced current [8]. The electromagnetic force resulting from the interaction of the EM field, and inductive eddy current lifts the sample [8]. Figure 1 depicts the principle of electromagnetic levitation.

Experimental Aspects

Design of Levitation Equipment

The electromagnetic levitation facility used in this work is shown in Fig. 2. The apparatus consists of a quartz tube chamber (15 mm O.D., 13 mm I.D., 304 mm length) a copper levitation coil wound using 1/8 in. diameter tubing, a rotatable platform housing a copper mold and alumina rod. Power is provided to the coil using an Ameritherm-Ambrell high frequency induction heating system with a rated terminal output of 10 kW and a frequency range from 150 to 400 kHz. Adjustment in applied current allows for the manipulation of the vertical position of the droplet within the levitation coil, and accordingly the amount of heating provided to the sample based on interaction with field flux lines. A minimum working current to support the droplet in levitation is dependent on sample material, mass, gas flow rate, and coil design.

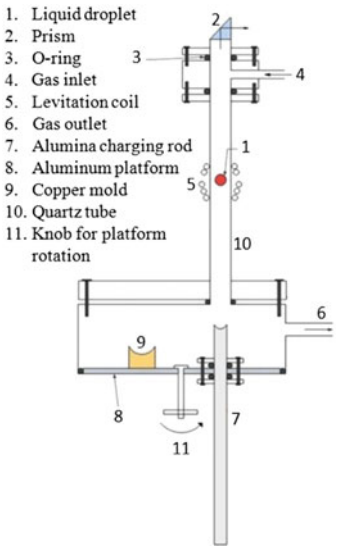

Fig. 2 Schematic diagram of EML apparatus

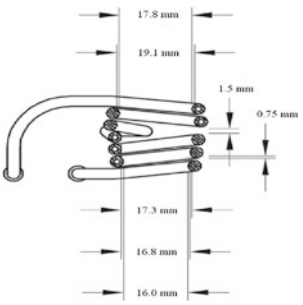

Fig. 3 Schematic diagram of levitation coil

Figure 3 shows a schematic of the five-turn levitation coil used in this work [10]. The coil is a low-angle conical configuration comprising two sections: a lower three-turn primary cone, and an upper inverted cone with two reverse turns. With this configuration, the lower cone serves to provide sufficient lifting force and droplet heating to appropriate temperature, while the upper inverted cone provides vertical and lateral stability of the droplet.

Temperature Measurement

Droplet temperatures were measured using a CHINO IR-CA Q3088 two-color pyrometer with an uncertainty of ±15 °C. The pyrometer is aimed on the droplet surface through the viewing window at the top of the levitation chamber and

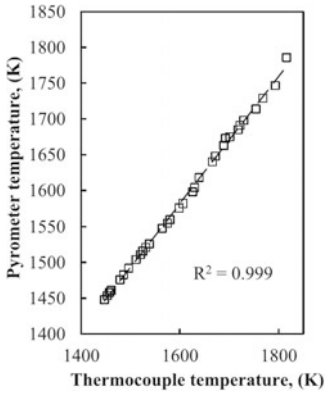

Fig. 4 Pyrometer calibration for molten iron by comparison with a submerged thermocouple

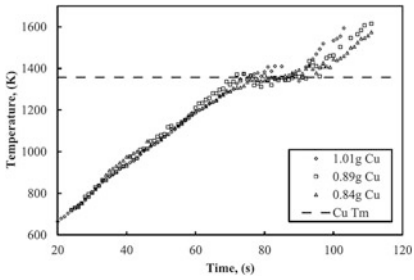

Fig. 5 Pyrometer calibration using levitated copper droplets of different mass

continuous temperature readings obtained. The optical viewing window serves to minimize spectral losses during measurements. Two separate pyrometer calibration tests were carried out. For the first test, measurements were taken from a thermocouple submerged in molten iron contained in a crucible located within an induction furnace under a hydrogen–argon atmosphere [10]. The melting point of iron was compared with the recorded measurements from both the thermocouple and the pyrometer (Fig. 4). For the second calibration test, the levitation furnace was used with copper droplets. The pyrometer calibration was verified by measuring the recorded melting temperatures of levitated copper droplets of different mass as shown in Fig. 5 [10].

Levitation of Silicon–Iron Alloys

Silicon–iron alloy samples were cut into 0.6–0.7 g (±0.01) sections. A specimen is placed on the alumina charging rod, and raised into the sealed levitation chamber to a position between the upper and lower cones of the coil. The chamber is purged with the reaction/inert gas mixture for 1–2 min and checked for leaks. With application of electrical power to the coil, the solid specimen levitates, generally at

temperatures of 1173–1273 K. The charging rod is retracted as soon as stable levitation of the solid specimen is obtained. The specimen usually melts within 1 min, and the temperature is adjusted to the required value by control of the applied current. After a given reaction time, the rotatable platform is turned so that the copper mold is positioned below the coil. When the power is turned off, the droplet falls and is quenched in the copper mold. The specimen is then recovered for subsequent analysis by inductively coupled plasma optical emission spectroscopy.

Results and Discussion

Effect of Time and Temperature

The results in Fig. 6 shows that phosphorus removal increases with both time and temperature. The rate of removal appears to follow first-order reaction kinetics. Steady state conditions are achieved after approximately 45 min, beyond which the concentration of phosphorus remains essentially constant. The higher processing temperature of 1993 K results in a lower final phosphorus content, with 72% of phosphorus removal achieved after levitation of a 25 wt%Fe–Si alloy with an initial P content of 0.025 wt% for 40 min in a 50%H_2–Ar mixture at 0.5 L/min flow rate. However processing at high temperatures is unfavorable from an energy standpoint. Furthermore, with the vapour pressure of silicon known to increase significantly at temperatures above the melting point, processing at higher temperature would result in silicon vaporization losses [11].

Effect of Hydrogen Partial Pressure

The effect of hydrogen concentration on dephosphorization behavior is shown in Fig. 7 for flow rates of 0.5 and 1.2 L/min. In both cases, a positive correlation

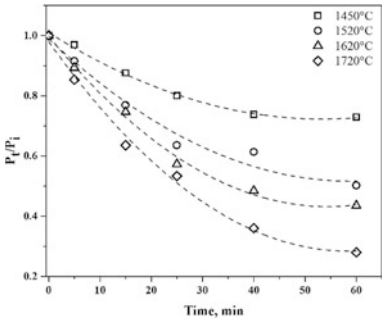

Fig. 6 Effect of time and temperature on dephosphorization with 50% H_2–Ar

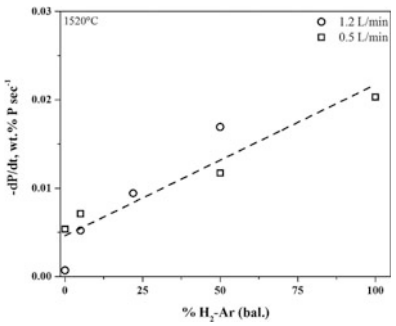

Fig. 7 Effect of H_2 concentration on dephosphorization

between a higher partial pressure of hydrogen and increased rate of dephosphorization is observed. The effect of gas flow rate for the range investigated does not appear to be significant. Further work is required to identify and quantify the reaction products in order to confirm the mechanism of phosphorus removal from silicon–iron alloys.

Effect of Iron Alloying

Based on the results shown in Fig. 8, increasing Fe content is observed to impede phosphorus removal. This effect is likely due to the stronger affinity of Fe for P, than Si for P, as indicated by the calculated iso-activities of P in the ternary Si–Fe–P system, Fig. 9, and work by Khajavi et al. [12]. In Fig. 9, the activity of P displays a large negative deviation from ideality. An increase in Fe content, or decrease in Si content is shown to increase the deviation of P activity from ideality, which is consistent with the observed affinity of P for Fe in Si–Fe melts.

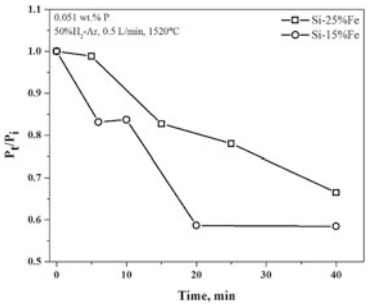

Fig. 8 Effect of Fe on dephosphorization

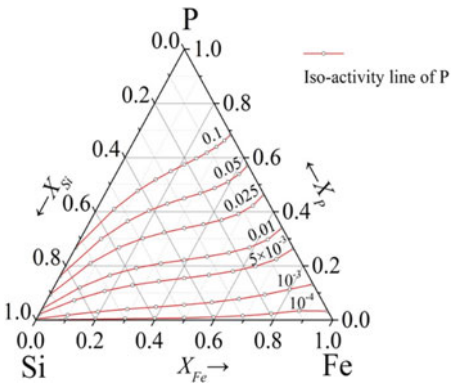

Fig. 9 Iso-activity curves of [P] in Si–Fe–P alloys

Effect of Initial Phosphorus Concentration

It is observed that a higher initial phosphorus concentration in the silicon alloy droplets results in a greater dephosphorization (Fig. 10). At lower initial phosphorus concentrations, and phosphorus depletion in the alloy melt as the reaction proceeds, the overall rate is expected to be controlled by mass transfer in the liquid metal. It is noteworthy that the dephosphorization rate for the higher initial phosphorus concentrations has promising implications for the refinement of high alloy steels. In such operations, strict control of alloying element contents including chromium, nickel, and silicon is critical. Under oxidizing conditions, the risk of alloying element loss is significant due to preferential oxidation compared with phosphorus. Accordingly, as demonstrated during the present work, refining of high-alloyed steels under a reducing environment would prevent alloy loss due to be oxidation.

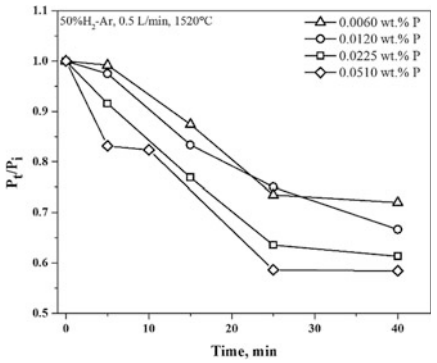

Fig. 10 Effect of initial phosphorus concentration on dephosphorization

Conclusions

Dephosphorization was achieved by electromagnetic levitation refining of silicon–iron alloys in H_2–Ar gas mixtures. The degree of dephosphorization was found to increase with reaction time, with 72% of phosphorus removed after 40 min at 1993 K in a 50%H_2–Ar mixture. However, processing at lower temperatures is expected to reduce evaporation losses of silicon and increase the process efficiency. Higher concentrations of hydrogen in the gas mixture as well as higher initial phosphorus concentration in the alloy were observed to increase dephosphorization. Increase of iron content in the silicon–iron alloys was found to lower the rate of phosphorus removal. Further work based on these preliminary findings could facilitate the development of an innovative technique for refining metallurgical grade silicon alloys and ultimately contribute to a cost effective route for the production of solar grade silicon.

Acknowledgements Appreciation is expressed to the Natural Sciences and Engineering Research Council of Canada for providing funding for this project through a Strategic Research Grant.

References

1. Monroe, J., & Wickander, R. (2006). *Essentials of geology* (4th ed.). Belmont, USA: The Thomson Corp.
2. Lynch, D. (2009). Winning the global race for solar silicon. *JOM Journal of the Minerals Metals and Materials Society, 61,* 41–48.
3. The International Renewable Energy Agency. (2013). Solar technology brief.
4. Johnston, M., Khajavi, L., Li, M., Sokhanvaran, S., & Barati, M. (2012). High-temperature refining of metallurgical-grade silicon: A review. *JOM Journal of the Minerals Metals and Materials Society, 64,* 935–944.
5. Ueda, S., Morita, K., & Sano, N. (1997). Thermodynamics of phosphorus in molten Si-Fe and Si-Mn alloys. *Metallurgical and Materials Transactions B, 28B,* 1151–1155.
6. Hino, M., & Ito, K. (2010). *Thermodynamic data for steelmaking*. Sendai, Japan: Tohoku University Press.
7. Hectors, D., Van Reusel, K., & Diesen, J. (2008). Experimental validation of electromagnectic-thermal coupled modelling of levitation melting. *Przeglad Elektrotechniczny, 84,* 140–143.
8. Asakuma, Y., Sakai, Y., Hahn, S., Tsukada, T., Matsumoto, T., Fujii, H., et al. (2000). Equilibrium shape of a molten silicon drop in an electromagnetic levitator in microgravity environment. *Metallurgical and Materials Transactions B, 31,* 327–329.
9. Popa, M. (2010). Study of an electromagnetic levitation system. *Nonconventional Technologies Review, 1,* 34–38.
10. Wu, P., Yang, Y., Barati, M., & McLean, A. (2014). Electromagnetic levitation of silicon and silicon-iron alloy droplets. *High Temperature Materials and Processes, 33*(1), 1–7.
11. Wei, K. X., Ma, W. H., Dai, Y. N., Yang, B., Liu, D. C., & Wang, J. F. (2007). Vacuum distillation refining of metallurgical grade silicon (I)—Thermodynamics on removal of phosphorus from metallurgical grade silicon. *Transactions of Nonferrous Metals Society of China, 17,* 1022–1025.
12. Khajavi, L. T., & Barati, M. (2012). Thermodynamics of phosphorus removal from silicon in solvent refining of silicon. *High Temperature Material Process, 31,* 627–631.